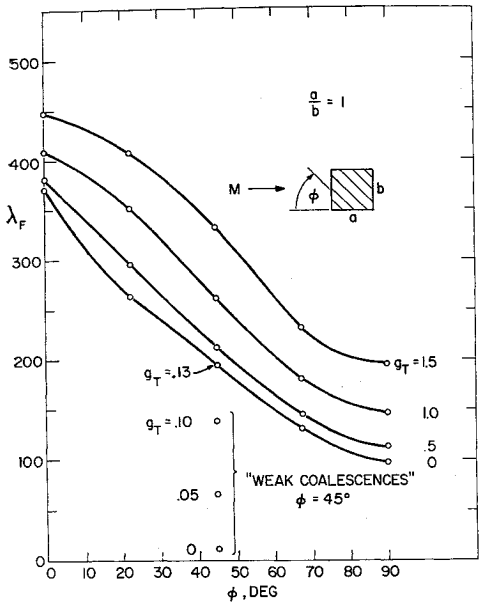

Fig. 4 Effect of angle of orthotropicity on flutter boundary.

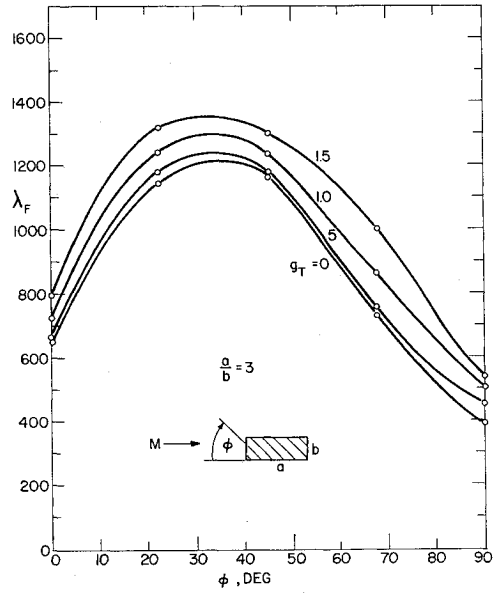

Fig. 5 Effect of angle of orthotropicity on flutter boundary.

angles may be preferred, depending primarily on a/b, amount of damping, and amount of orthotropicity present.

This investigation has limitations at high a/b. A more refined aerodynamic surface theory should be used there, because of low aspect ratio effects. Secondly, more deflection modes should be used to improve convergence because of the "membrane-like" behavior at high a/b. Qualitative trends, however, may still be revealed.

References

[1] Calligeros, J. M. and Dugundji, J., "Supersonic flutter of rectangular orthotropic panels with arbitrary orientation of orthotropicity," TR 74-5, Mass. Inst. Tech. Aeroelastic and Structures Res. Lab. (June 1963).

[2] Hedgepeth, J. M., "Flutter of rectangular simply supported panels at high supersonic speeds," J. Aeronaut. Sci. 24, 563–573 (1957).

[3] Hearmon, R. F. S., *An Introduction to Applied Anisotropic Elasticity* (Oxford University Press, London, 1961), Chap. VII, p. 94.

[4] Movchan, A. A., "On the stability of a panel moving in a gas," NASA RE 11-21-58W (1959).

Rapid Discharge of a Gas from a Cylindrical Vessel through a Nozzle

R. C. Progelhof* and J. A. Owczarek†
Lehigh University, Bethlehem, Pa.

Nomenclature

a = speed of sound
A = cross-sectional area
d = diameter of nozzle throat
L = length of cylindrical vessel
p = pressure
t = time
u = magnitude of the flow velocity
x = distance
δ^* = boundary-layer displacement thickness
γ = ratio of specific heats

Subscripts

0 = initial conditions
e = exit of nozzle
f = minimum cross-sectional area of flow stream
v = vessel

Introduction

THIS note is a continuation of the investigation on the rapid discharge of a gas from a cylindrical vessel made by the authors.[6] The constrictive devices used in these experiments were standard American Society of Mechanical Engineers long-radius flow nozzles with β ratios of approximately 0.25, 0.50, and 0.66. The experimental equipment and technique are identical to those of the previous investigation on the discharge with orifice constrictions. Figure 1 is a comparison of three oscilloscope traces for the same pressure ratio but with different nozzles. It shows how sensitive the variation of pressure with time in the vessel is to the exit area of the nozzle.

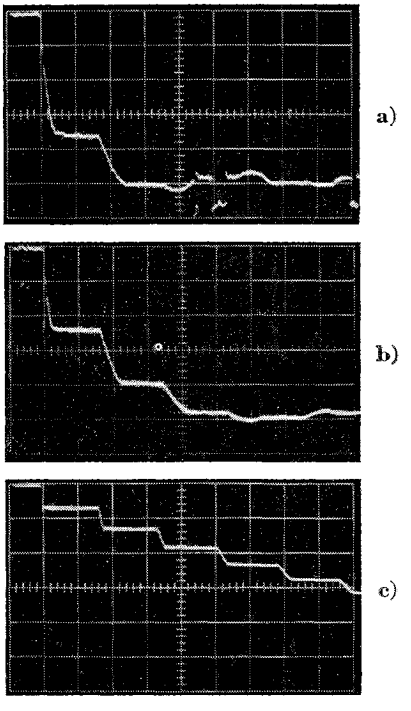

Fig. 1 Pressure record at the sealed end of the vessel, X/L = 0, for the same initial pressure, 30 psia, and oscilloscope settings with nozzle β ratios of a) 0.66, b) 0.50, and c) 0.25.

Received July 10, 1963.

* Assistant Professor, Department of Mechanical Engineering.
† Associate Professor, Department of Mechanical Engineering.

The experimental results are compared on Fig. 2c with the pressure-time variation predicted by the method of characteristics based on the physical area of the nozzle and assuming that the flow is quasi-steady within the nozzle and that the pressure equalization in the exit plane is instantaneous.[3] The quasi-steady flow continuity and energy equations relate the flow functions of the gas at the inlet to the nozzle, a/a_0 and u/a_0, to the ratio of the exit area of the nozzle to the cross-sectional area of the vessel, ϕ, and to the ratio a_e'/a_0, where a_0 is a reference speed of sound taken as the speed of sound of the gas in the vessel before the discharge and a_e' denotes the speed of sound of the gas before the discharge if it were expanded in a reversible adiabatic process.[3,4]

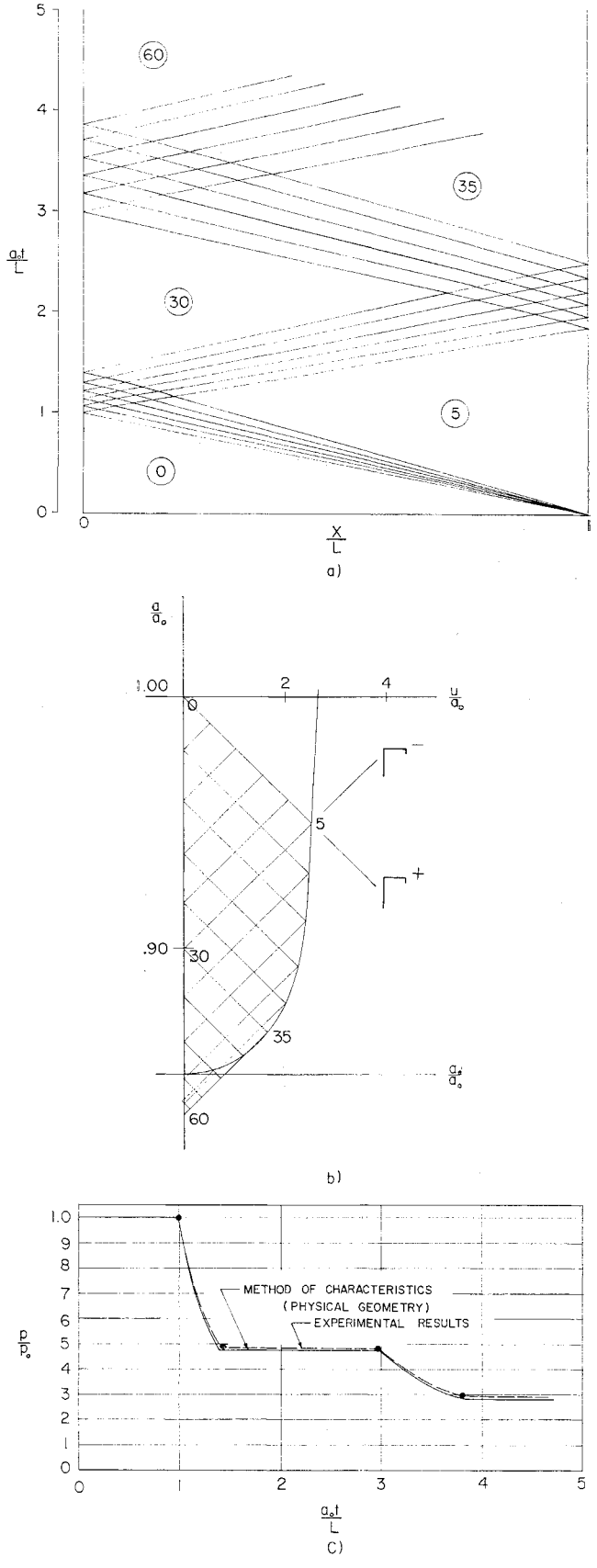

Fig. 2 Graphical solution and a comparison of theoretical and experimental results for $\phi = 0.44$ and $a_e'/a_0 = 0.35$.

The variation of the flow functions u and a of the gas across the initial expansion wave entering the vessel lies in the state plane on the Γ^+ characteristic, $du/da = -2/(\gamma - 1)$, passing through point 0 shown on Fig. 2b. The strength of the wave is fixed by the area ratio ϕ and is determined by the intersection of the characteristic and the ϕ = const boundary condition, point 5. The variation of the flow functions of the gas across the expansion wave reflected from the sealed end of the vessel lies on a Γ^- characteristic, $du/da = 2/(\gamma - 1)$, passing through point 5. The strength of the reflected wave is fixed by the boundary condition requiring zero flow velocity at the sealed end, point 30. The initial pressure drop at the sealed end, Δp, can be calculated from the homentropic flow relationship between the speed of sound a/a_0 and the pressure ratio p/p_0. Reversing the technique just described, from the experimentally determined pressure drop one can determine the effective contraction ratio $\bar{\phi}$ under the assumption that the gas is expanded in a homentropic one-dimensional unsteady discharge process. Such calculations were repeated for successive pressure drops and the experimental results put in a more convenient form of a contraction coefficient Λ defined as follows:

$$\Lambda = \bar{\phi}/\phi = A_f/A_e$$

Analysis of Results

Assuming the one-dimensional approximation to hold and neglecting the heat transfer and viscous effects inside the vessel, the discrepancies between the observed and calculated results, which are very small, can be attributed mainly to the boundary-layer growth inside the nozzle. To the first approximation the boundary-layer growth inside the nozzle can be considered to correspond to the boundary-layer growth on a flat plate.[2,7,8] The length of the equivalent flat plate, based on the results obtained by Simmons,[8] was assumed to be equal to a quarter of the major axis of the ellipse forming the converging section of the nozzle plus the length

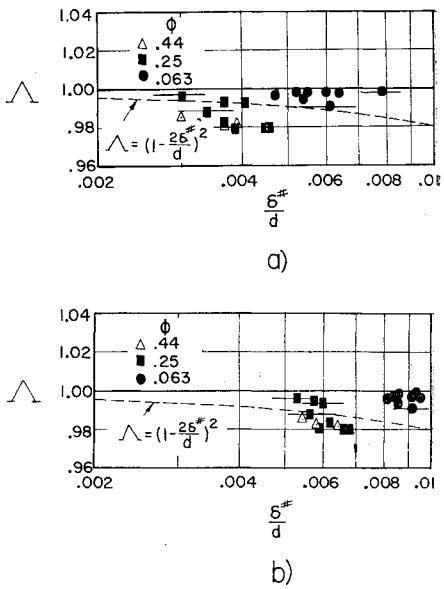

Fig. 3 A comparison of experimentally determined effective contraction ratios with those obtained from a flat-plate boundary-layer approximation; a) laminar, b) turbulent.

of the straight section of the nozzle. The laminar boundary-layer displacement thickness, including the effects of compressibility and deceleration of the freestreams, was calculated from the results presented by Moore.[5] The turbulent boundary-layer displacement thickness was calculated for an incompressible fluid. However, the effects of compressibility were estimated from the work of Cope[1] and were found to have a relatively small effect on δ^*/d in the range of conditions tested. In the experiments performed, the Reynolds numbers based on the equivalent flat plate length ranged from 0.5 to 2.5 $\times$ 10^6. The experimentally determined effective contraction ratios are plotted in Figs. 3a and 3b for laminar and turbulent boundary-layer growth on the equivalent flat plate, respectively. The effect of the assumption on the equivalent flat-plate length for the converging section of the nozzle is also indicated for several points in Fig. 3 by assuming the length equal to $\frac{1}{8}$ and $\frac{3}{8}$ of the major axis.

Conclusions

For the range of conditions covered, the experimental results indicate that the pressure variation inside the vessel can be closely approximated by assuming that the flow is one-dimensional and quasi-steady within the nozzle and that the discharge area is equal to the physical area of the nozzle.

References

[1] Cope, W., *Modern Developments in Fluid Dynamics, High Speed Flow*, edited by L. Howarth (Oxford University Press, London, 1953), Vol. 1, pp. 456–462.

[2] Hall, G. W., "Application of boundary layer theory to explain some nozzle and venturi peculiarities," Proc. Inst. Mech. Engrs. **173**, 837–870 (1959).

[3] de Haller, P., "On a graphical method of gas dynamics," Sulzer Tech. Rev. **1**, 6–24 (1945).

[4] Kestin, J. and Glass, J. S., "The rapid discharge of a gas from vessels," Aircraft Eng. **23**, 300–304 (1951).

[5] Moore, F. K., "Unsteady laminar boundary layer flow," NACA TN 2471 (1951).

[6] Progelhof, R. C. and Owczarek, J. A., "The rapid dishcarge of a gas from a cylindrical vessel through an orifice," Am. Soc. Mech. Engrs. Paper 63-WA-10 (1963).

[7] Schlichting, H., *Boundary Layer Theory* (McGraw Hill Book Co. Inc., New York, 1960), Chap. 7, 15, 21.

[8] Simmons, F. G., "Analytical determination of the discharge coefficients of flow nozzles," NACA TN 3447 (1955).

Far Infrared Radiation Model of the Earth

ROBERT A. MCGEE*
General Electric Company, Utica, N. Y.

Introduction

MANY space vehicles contain equipment to sense infrared radiation from the earth. The spectral region from 7 to 13 μ, in which the atmosphere is quite transparent, has been very popular for such equipment. At wavelengths below 2 μ, reflection of sunlight becomes a problem, and at longer wavelengths the choice of detectors and optical materials is quite limited. Germanium has been a common choice of optical material because of its high transmission in the 3- to 16-μ region and its desirable mechanical properties, and thermistor bolometers have been favored as detectors.[4] This combination lends itself to equipments using the 7- to 13-μ atmospheric window. Recent experiments, such as the Tiros radiation experiments, however, have indicated that the radiation from the earth is highly variable in this spectral region. As a result, a study has been undertaken to determine the cause and to predict the types of variation to be expected. An analytical model was developed, and the results predicted by this model have been compared with data from the Tiros radiation experiments.

Presented at the IAS National Summer Meeting, Los Angeles, Calif., June 19–22, 1962; revision received July 18, 1963.

* Engineer, Light Military Electronics Department.

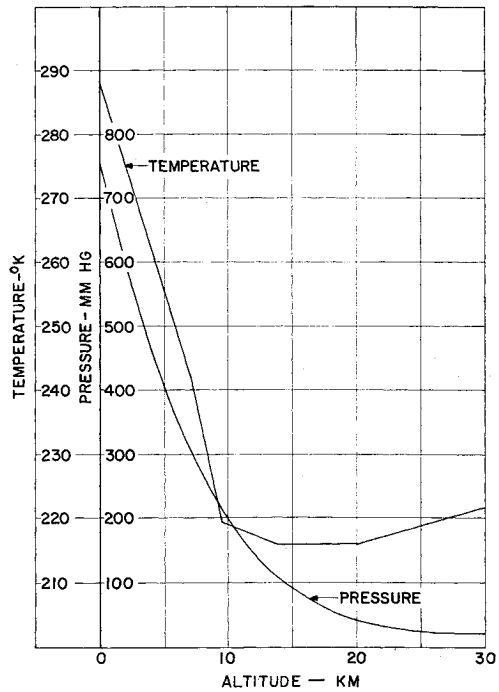

Fig. 1 Temperature and pressure profiles.

Description of Model

The earth's atmosphere is composed of a number of gases, each of which selectively absorbs radiation transmitted through it. The absorption through any gas is a function of the amount of gas present, its temperature and pressure, and the wavelength of the transmitted radiation. The constituents that absorb infrared radiation appreciably are water vapor, carbon dioxide, ozone, and nitrous oxide. Once the amount of each constituent in a given path has been determined, the total transmission through the path as a function of wavelength may be found. The mathematical procedure

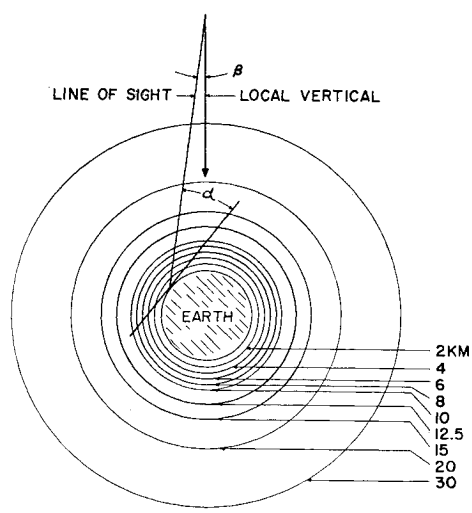

Fig. 2 Physical model and geometry.